ROBUST DESIGN FOR AEROELASTICALLY TAILORED / ACTIVE AEROELASTIC WING

P. Scott Zink*, Dimitri N. Mavris†
Georgia Institute of Technology, Atlanta, Georgia

Michael H. Love‡
Lockheed Martin Tactical Aircraft Systems, Ft. Worth, Texas

Mordechay Karpel§
Technion - Israel Institute of Technology, Haifa, Israel

Abstract

A study of multidisciplinary design concerning the incorporation of aeroelastic tailoring, control surface blending, and active aeroelastic wing concepts is presented. The design process incorporates response surfaces, fast probability integration and modal-basis multidisciplinary design optimization to characterize the design space. The wing box skins of a representative fighter configuration with multiple wing control surfaces are sized to minimum weight. A design of experiments approach is developed for the gear ratios in control surface blending. Design optimization is conducted for each set of gearing functions. The control surface gear ratios are then treated as “noise” in the structural design process, and a robust structural design is sought to account for the change in control laws that historically occur during the aircraft design process. The motivation for this methodology investigation is derived from the common occurrence of control law changes throughout the lifetime of an aircraft.

Introduction

Aeroelastic tailoring and active aeroelastic wing technologies are envisioned for application in the structural design of future advanced fighter aircraft with the goals of reducing weight and increasing maneuverability. Aeroelastic tailoring is the concept of using the directional stiffness properties of composites to design an aircraft structural component to deform under load in such a way as to benefit the performance of the aircraft. For example, Bohlmann, Eckstrom, and Weisshaar proposed aeroelastic tailoring for an oblique wing concept[1]. In this case structural wash-out of the forward swept part of the wing was used to counteract the 'natural', untailored tendency of that part of the wing to wash-in, while structural wash-in of the aft swept part of the wing was used to counteract the 'natural', untailored tendency of that part of the wing to wash-out thus providing a lateral load balance. They discovered that some of the benefits of aeroelastic tailoring included reduced aileron deflection required for trim and reduced hinge moments thus reducing required actuator weight and power[1]. Active aeroelastic wing (AAW) technology, which has recently been a key area of study for both the government and industry, as defined by Pendleton et. al., is "a multidisciplinary, synergistic technology that integrates air vehicle aerodynamics, active controls, and structures together to maximize air vehicle performance"[2]. AAW technology uses leading and trailing edge control surfaces to twist the wing which then becomes the primary surface for generating control power. As a result, wing flexibility is seen as an advantage rather than a detriment since the aircraft can be operated beyond reversal speeds and still generate the required control power for maneuvers. Since the AAW is more flexible than a comparable traditional wing, it has a lower weight[2].

Because aeroelastic tailoring and AAW technologies drive wing deformation to some desirable shape, they are complementary technologies that in combination should produce significant weight savings over untailored, traditionally controlled aircraft. Since both technologies are "multidisciplinary and synergistic" in nature it is important to consider their impact from the outset of the design process. This in and of itself presents a challenge since application of the technologies, particularly AAW technology, require detailed information of the structure, aerodynamics, and controls of the aircraft. In the beginning of the design process this kind of detailed knowledge is limited.

Much effort is being expended within the aerospace research community in establishing design knowledge early in the design process while at the same time keeping design freedom open. As examples, References 3 and 4 used finite element method and equivalent laminated plate analysis, respectively, in conjunction with a Design of Experiments/Response Surface Methodology (DOE/RSM) to generate wing weight response surface equations as a function of wing geometry. These equations were then incorporated into

---

* Graduate Research Assistant, Student Member AIAA
† Assistant Professor, Aerospace Engineering, Senior Member AIAA
‡ Senior Engineering Specialist, Senior Member AIAA
§ Associate Professor, Aerospace Engineering, Member AIAA

Copyright © 1998 by Lockheed Martin Corporation. Published by the American Institute of Aeronautics and Astronautics, Inc. with permission.

a synthesis/sizing code to replace the historically based equations that were being used in the code. Both of these references involved studies of the high speed civil transport (HSCT), an aircraft with very few historical counterparts. As a result, the historical weight equations in the code were questionable thus motivating a need for a more physics-based weight equation.

The early development of design knowledge (e.g. finite element models, CFD models in conceptual design) results in informed design decisions, but regardless of the speed of computers or the detail of the simulations, there will likely be inaccuracies over the course of the design that will require modifications. As a result, a challenge exists to acquire aircraft designs that are invariant to these prediction inaccuracies but that do not suffer severe performance and weight penalties. In consideration of aeroelastic tailoring and AAW, development of a structural design robust to aeroelastic load inaccuracies is desirable. A key constituent of the active aeroelastic wing concept is the control surface gear ratios (ratios that dictate how the control surfaces move with respect to a single basis control surface, Figure 1). The aeroelastic load is directly affected by the values of these gear ratios. Thus, a methodology is required to characterize the AAW design space so that aeroelastically tailored structural designs robust to changes in the gear ratios may be determined.

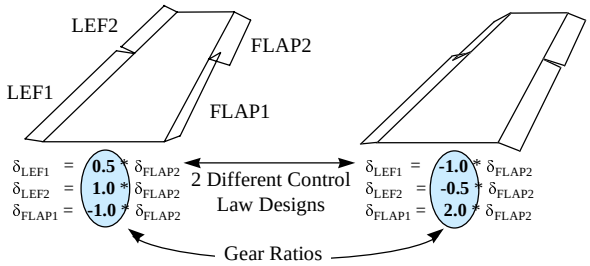

Figure 1 - Gear Ratio Illustration

Historically, design methodology for AAW[2] has comprised a direct gradient-based design optimization formulation in which the sensitivities and constraints of strength and control power are considered for a minimum weight objective. At the optimum weight design, the structural definition is assumed to be established. The robustness of the structural design, however, with respect to the inevitable change in gearing ratios (determined from this process) is unknown.

This paper discusses a robust design methodology for AAW. Since AAW technology exploits the use of multi-input, multi-output control surfaces there will be several gear ratios for each configuration. As a result, an optimal aeroelastically tailored configuration (e.g. the percentage of 0°, ±45°, 90° plies for each section of the wing) which gives the lowest wing weight will correspond to a unique set of gear ratios. If the gear ratios change, then the optimal tailoring configuration will change, and thus the weight will change. This study will seek to understand the relationship between gear ratios and weight through DOE/RSM techniques. Using these techniques one can then find the set of gear ratios that produces the lowest weight structure. However, this study is seeking not only to find the lowest weight wing structural configuration, but also to find the configuration that is low weight *and* invariant (i.e., *robust*) to small changes in the gear ratios. The motivation for this methodology investigation is derived from the common occurrence of control law changes throughout the lifetime of an aircraft.

Tools

ASTROS Modal Approach

At the core of this methodology is an aeroelastic sizing tool that operates in a timely manner for the DOE/RSM approach. A modal approach to aeroelastic analysis and optimization has been developed and incorporated into the Lockheed Martin version of ASTROS[5,6]. This approach provides finite element methods in a computationally efficient and accurate manner. Reference 6 discusses the formulation of the modal approach for analysis and optimization. At the heart of this formulation is the use of several low frequency modes of vibration of the structure to create generalized stiffness and force matrices for static analysis and optimization. Thus, the size of the problem can be reduced significantly, since with the discrete approach, the number of degrees of freedom may number in the several thousands. The structural displacements, after the reduced equations of motion have been solved, are then expressed as a linear combination of the baseline modes which served as the generalized coordinates. Table 1 shows a comparison of convergence histories for a structural optimization in ASTROS from this study using the modal approach and the discrete approach. The discrete approach model contains 3762 degrees of freedom, and the modal approach model uses 50 mode shapes as the generalized coordinates.

Table 1 - Convergence History Comparison

Iteration	Modal (Weight, lb)	Discrete (Weight, lb)
1	404.82	404.82
2	580.70	496.01
3	445.21	377.47
4	344.93	337.41
5	314.65	310.85
6	307.57	307.02
7	306.93	301.75
8	302.44	301.17
9	301.71	301.02
10	301.52	300.81
11	298.45	297.46
12	298.22	**297.63**
13	**298.23**	
CPU Time:	**00:57:42.4**	**03:17:24.2**

Design of Experiments/Response Surface Methodology

The DOE/RSM techniques used to understand the relationship between wing weight and gear ratio values employs intelligent design of experiments and statistical multivariate regression to relate a response to a set of contributing variables[7]. Many times the relationship between the response and the design variables is either too complex or unknown, so that it becomes necessary to use an empirical approach to build an approximate model of the exact relationship. The model, for the purposes of this study, is a 2nd order equation, also referred to as a response surface equation (RSE), and takes the following form:

$$R = b_0 + \sum_{i=1}^{k} b_i x_i + \sum_{i=1}^{k} b_{ii} x_i^2 + \sum_{i=1}^{k-1} \sum_{j=i+1}^{k} b_{ij} x_i x_j \qquad (1)$$

where,

b_i are coefficients for the first degree terms

b_{ii} are coefficients for the pure quadratic terms

b_{ij} are the coefficients for the cross-product terms

These coefficients are estimated using least squares regression of experimental or computer simulated data, which is provided in an organized manner through a design of experiments[7].

After checking the validity of the RSE within the designated design space and making sure that it fits reasonably well the data that was used to create it, the designer then has a convenient model in which to gain visibility of what might be a very complex design space. It is precisely this visibility that gives DOE/RSM an advantage over traditional optimization routines, particularly in a conceptual design setting where design "openness" is desirable.

The Advanced Mean Value Method

Since this paper will be investigating a methodology to determine robust structural designs, a tool that is capable of modeling random variables is necessary. The Advanced Mean Value (AMV) method is used to fill the role for this part of the study. The AMV method is an option in the Fast Probability Integration (FPI) computer program[8] and is used to estimate a cumulative probability distribution function of a response given that its contributing variables are probabilistic according to user-defined distributions. For example, the AMV method was used in Reference 9 to find the approximate cumulative distribution function (CDF) of required average yield per revenue passenger mile. In this case, FLOPS/ALCCA, a sizing/synthesis/economic analysis code, was used to size an HSCT concept. Input variables, such as design range, wing area, and fuel cost, were treated probabilistically. The primary advantage of the AMV method is that the number of runs of the analysis code in generating the CDF for a desired response is kept to a reasonable level. However, with a Monte-Carlo simulation, which is the more exact and accurate way to generate a CDF, the number of computer runs could number near 10,000, an unreasonable number of runs particularly for finite element analysis. Although the AMV method is an approximation to the CDF, Reference 10 showed that for a sizing/synthesis/economic analysis problem of an HSCT with random input variables, the CDF produced by the AMV method matched well that produced by a Monte-Carlo simulation.

Reference 8 discusses in detail the theoretical development of the AMV method. The AMV method first assumes the response function (referred to as a Z-function in FPI literature) to be smooth and that a Taylor series expansion of the following form exists at the mean of the input variables (**X**):

$$Z(\mathbf{X}) = Z(\mu) + \sum_{i=1}^{n} \left(\frac{\partial Z}{\partial X_i} \right) \cdot \left(X_i - \mu_i \right) + H(\mathbf{X}) \qquad (2)$$

$$= a_0 + \sum_{i=1}^{n} a_i X_i + H(\mathbf{X}) \qquad (3)$$

$$= Z_{mv}(\mathbf{X}) + H(\mathbf{X}) \qquad (4)$$

The coefficients of the Taylor series expansion, a_i, are obtained by numerical differentiation. If the response function was relatively linear then the higher order terms H(**X**) could be neglected. In this case, if the input variables are normally distributed, then the mean and variance of the linearized response function

(Z_{mv}(**X**)) can be found using the additive property of normal distributions as given below[11]:

$$\mu_Z = a_0 + \sum_{i=1}^{n} a_i \mu_{x_i} \tag{5}$$

$$\sigma_Z^2 = \sum_{i=1}^{n} a_i^2 \sigma_{X_i}^2 \tag{6}$$

However, if the Z-function is nonlinear, then an additional step is necessary to approximate the influence of the higher order terms (H(**X**)) on the CDF of the response function. It is the problem of nonlinearity that the AMV method attempts to address by using a simple correction procedure on the linear assumption. The correction procedure involves estimating the function value for a user-defined set of CDF values (referred to as P-levels) based on the linear function, Z_{mv}. Figure 2 illustrates some of these concepts including the AMV correction and the user defined P-levels.

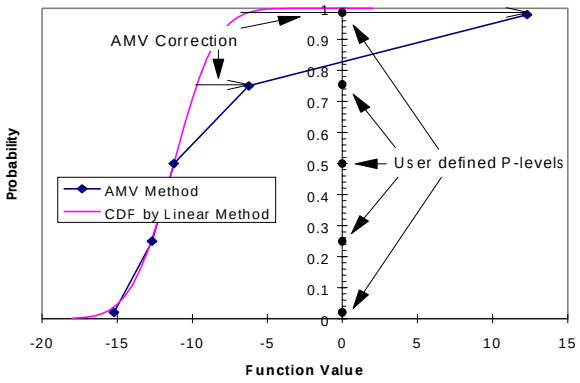

Figure 2 - AMV Illustration

The number of function evaluations necessary to generate a CDF using the AMV method include:

1) **n + 1** where n = number of input variables
2) **m** where m = number of user-defined P-levels

The first set of function calls is to calculate the Taylor series coefficients (a_i), and the second set of calls is required to perform the AMV correction at each of the specified P-levels. Thus, by using the AMV method n+1+m functional calls are required, providing significant time savings over a traditional Monte-Carlo approach.

ASTROS Model

Figure 3 shows the ASTROS structural model being used in this study. It is a preliminary design finite element model of an advanced fighter composite aircraft with 4 wing control surfaces (2 trailing edge, 2 leading edge) and a horizontal tail. The skins of the wing are made up of 4 composite orientations, 0°, ±45°, and 90° plies, where the thickness of the -45° and +45° orientations are constrained to be equal. The 0° plies are oriented approximately parallel to the wing box leading edge spar. In addition, the composite wing skins are designed (*tailored*) in thickness and percentage of thickness to orientations, via ASTROS optimization routines, for specified maneuver and strength requirements[12]. The number of discrete degrees of freedom is 3762, and 51 modes for the symmetric analyses and 50 modes for the antisymmetric analyses are used for the modal approach.

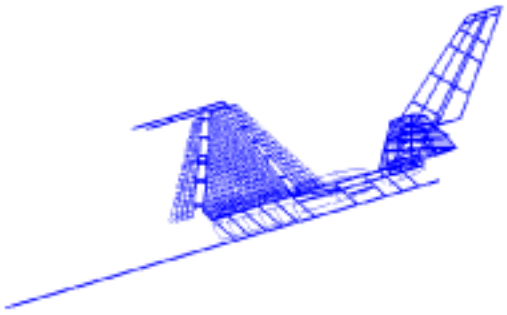

Figure 3-- Structural Model

The aerodynamic model is shown in Figure 4. It is a flat panel Carmichael[13] model containing 143 vertical panels and 262 horizontal panels. ASTROS has been modified to allow inclusion of Carmichael panel geometry and aerodynamic influence coefficients which then replace the existing aerodynamic database entities created by USSAERO, ASTROS original aerodynamics module. Carmichael results are produced for two Mach numbers, 1.2 and 0.95, for both symmetric and antisymmetric conditions[12].

Figure 4 -- Aerodynamic Model

The design variables in the ASTROS optimization for this model are the layer thickness of the composite skins. The number of design variables is 78 due to physical linking of the skin elements. Internal structure

and carry-thru structure remain fixed for this study. Table 2 shows the maneuver conditions and strength constraints to which the structure is designed.

Table 2 - Maneuver Conditions and Design Constraints

Maneuver Condition	Design Constraint
1) Mach 0.95, 10,000 ft 9g, Pull-Up	fiber strain: 3000 με tension 2800 με compression
2) Mach 1.20, Sea Level -3g, Push-Over	fiber strain: 3000 με tension 2800 με compression
3) Mach 1.20, Sea Level Steady State Roll = 100^{O}/s	fiber strain: 1000 με tension 900 με compression
4) Mach 0.95, 10,000 ft Steady State Roll = 180^{O}/s	fiber strain: 1000 με tension 900 με compression

For each maneuver, the deflections of 4 of the 5 control surfaces are linked to the remaining surface (known as a *basis surface*) via the gear ratios defined in the CONLINK bulk data card. This basis surface then is the free variable in the ASTROS trim module and the deflection of all other surfaces are dependent upon it. Table 3 shows the basis surfaces that were selected for each maneuver.

Table 3 - Basis Control Surfaces

Maneuver	Basis Surface
1	Horizontal Tail
2	Horizontal Tail
3	Outboard Leading Edge Flap
4	Outboard Aileron

The horizontal tail was selected for Maneuvers 1 & 2, since it has historically been the primary control surface for symmetric trim. The outboard leading edge surface was selected for Maneuver 3, because it is the most effective surface at supersonic conditions. Both trailing edge surfaces experience control reversal at supersonic flight, thus quickly ruling them out as candidates for the basis surface of Maneuver 3. The AAW concept incorporates the outboard leading edge flap for such cases. For Maneuver 4, the outboard aileron was chosen, since it is the most effective roll control surface at subsonic speeds.

Robust Aeroelastic Wing Design Method

The objective of this study is to find aeroelastically tailored structural designs that are robust to changes in the gear ratios. These tailored designs, in turn, are characterized by a unique set of gear ratios. This presents somewhat of a unique challenge in that the gear ratios are both control variables (variables over which the designer has control) and noise variables (variables over which the designer has no control) depending on the point in the design process.

Before the structure is initially sized, the structures design team, has to make some assumptions about the gear ratios and establish initial values for them. In this case they act as control factors, since the team can directly affect them, and then size the structure accordingly.

As the design process progresses and more detailed analyses or even flight tests are performed, stability and control engineers often discover that the gear ratios need to change. This change may be required due to maneuver performance, subsystem overload, or structural overload. In this case, from the structural designer's perspective, the gear ratios act as noise factors. This problem characteristic differs somewhat from previous work in robust design in which the control factors and noise factors were independent[14]. As a result, a modified methodology for robust design is required, and is hereby documented with application to the advanced fighter model.

Design Space Definition

The first phase of this methodology is the understanding of how the structural designs are characterized by the gear ratios. This requires building relationships between structural responses, such as designed structural weight and hinge moments, and the gear ratios.

The gear ratios that this study will be examining and the ranges of each are defined in Table 4. Since there are four maneuvers to which the structure is sized, and four gear ratios per maneuver, there are a total of 16 gear ratios that are of interest. The range of each gear ratio was established in part by the maximum and minimum deflection of the control surface to which it corresponds.

The responses of interest are listed in Table 5 as well as their notation that will be used throughout the remainder of the paper.

Table 4 - Design Variables and Ranges

Design Variable Name	Corresponding Surface	Maneuver	Min.	Max.
XLEF1_1	Inboard L.E.	Subsonic Pull-Up	-1.0	0.4
XLEF2_1	Outboard L.E.	Subsonic Pull-Up	-1.0	0.4
XFLAP1_1	Inboard T.E.	Subsonic Pull-Up	-1.0	1.0
XFLAP2_1	Outboard T.E.	Subsonic Pull-Up	-1.0	1.0
XLEF1_2	Inboard L.E.	Super. Push-Over	-1.0	0.4
XLEF2_2	Outboard L.E.	Super. Push-Over	-1.0	0.4
XFLAP1_2	Inboard T.E.	Super. Push-Over	-1.0	1.0
XFLAP2_2	Outboard T.E.	Super. Push-Over	-1.0	1.0
XTAIL_3	Horiz. Tail	Supersonic Roll	-0.065	2.0
XLEFA1_3	Inboard L.E.	Supersonic Roll	-0.16	2.0
XAILER1_3	Inboard T.E.	Supersonic Roll	-2.0	0.16
XAILER2_3	Outboard T.E.	Supersonic Roll	-2.0	0.16
XTAIL_4	Horiz. Tail	Subsonic Roll	-0.08	1.0
XLEFA1_4	Inboard L.E.	Subsonic Roll	-0.22	0.4
XLEFA2_4	Outboard L.E.	Subsonic Roll	-0.22	0.5
XAILER1_4	Inboard T.E.	Subsonic Roll	-0.22	2.0

Table 5 - Responses and Notation

Response	Notation	Unit
Designed Structural Wing Weight	Weight	lb
Maneuver 1 Drag	Drag1	lb
Maneuver 2 Drag	Drag2	lb
Hinge Moment LEF1 - Maneuver 1	HM_LEF1_1	lb-in
Hinge Moment LEF2 - Maneuver 1	HM_LEF2_1	lb-in
Hinge Moment FLAP1 - Maneuver 1	HM_FLAP1_1	lb-in
Hinge Moment FLAP2 - Maneuver 1	HM_FLAP2_1	lb-in
Hinge Moment LEF1 - Maneuver 2	HM_LEF1_2	lb-in
Hinge Moment LEF2 - Maneuver 2	HM_LEF2_2	lb-in
Hinge Moment FLAP1 - Maneuver 2	HM_FLAP1_2	lb-in
Hinge Moment FLAP2 - Maneuver 2	HM_FLAP2_2	lb-in
Hinge Moment LEFA1 - Maneuver 3	HM_LEFA1_3	lb-in
Hinge Moment LEFA2 - Maneuver 3	HM_LEFA2_3	lb-in
Hinge Moment AILER1 - Maneuver 3	HM_AILER1_3	lb-in
Hinge Moment AILER2 - Maneuver 3	HM_AILER2_3	lb-in
Hinge Moment LEFA1 - Maneuver 4	HM_LEFA1_4	lb-in
Hinge Moment LEFA2- Maneuver 4	HM_LEFA2_4	lb-in
Hinge Moment AILER1 - Maneuver 4	HM_AILER1_4	lb-in
Hinge Moment AILER2 - Maneuver 4	HM_AILER2_4	lb-in

Of all the responses, the structural weight is the most important because it does the best job of capturing the overall "goodness" of the structural design. The drag for each symmetric maneuver is being evaluated because it provides some indication of the aerodynamic "goodness" of the structural design. The hinge moments are important, because they directly affect actuator weight and power. In fact, given a fixed actuator with maximum allowable moment, the hinge moment responses can be considered as constraints in the design space.

Screening Test

As discussed in a previous section, the relationships between structural characteristics and gear ratios are approximated by RSEs using DOE/RSM techniques. However, the 16 design variables (gear ratios) delineated in Table 4 is a sizable design space to manage. Thus, it is desirable to screen out some variables to reduce the size of the problem to a manageable level, while at the same time acknowledging that many of the variables will be relatively insignificant.

The screening test is a 128 case, 2-level fractional factorial DOE , meaning that each gear ratio is tested only at its minimum and maximum value. The DOE is built using the statistical software, JMP[15], and a sample of the screening test is shown in Table 6 where the +1 refers to the maximum value of the gear ratio and -1, to its minimum value. Each row of the DOE corresponds to an experiment, where each experiment is an ASTROS optimization run with different gear ratio values. As a result, each row also corresponds to a different structural design where laminate thickness and percent layer thickness of the structure are different from case to case. For each of these optimizations, designed wing weight is extracted and inserted into the response column of the DOE table.

Table 6 - Sample of Screening Test

	XLEF1_1	XLEF2_1	···	XLEFA2_	XAILER1_4	Weight
1	-1	-1	···	1	-1	319.7
2	-1	-1	···	1	1	312.7
3	-1	-1	···	-1	-1	344.0
4	-1	-1	···	-1	1	308.4
5	-1	-1	···	1	1	303.2
. .	. .	. .	. .	. .	. .	. .
124	1	1	···	1	-1	300.1
125	1	1	···	-1	-1	292.1
126	1	1	···	-1	1	347.3
127	1	1	···	1	-1	342.5
128	1	1	···	1	1	285.8

Within JMP an effect screening is then performed on the extracted data to determine which variables contribute most to wing weight. For this case, the effect screening involves a linear regression of the weight using only main effect terms (e.g., XLEF1_1) and 2nd order interaction terms (e.g., XLEF1_1*XLEF2_1). The regression coefficients of each of these terms is then scaled and graphed in descending order on a plot known as a Pareto plot (Figure 5). The length of the bar for each effect is equal to the absolute value of its scaled estimate divided by the sum of the absolute value of all scaled estimates. It is, in essence, the effect's percent contribution to the predicted value of weight[15].

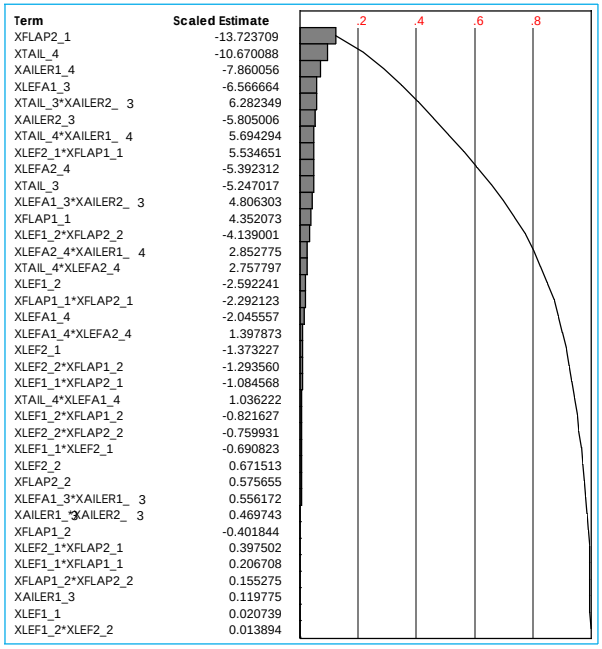

Figure 5 - Pareto Plot from Screening Test

The 8 most significant gear ratios from the screening test are shown in Table 7. These gear ratios were selected based on the order of their appearance in the Pareto plot. The other 8 gear ratios that were not particularly significant then were set to their midpoint values and remained fixed for the remainder of the study.

Table 7 - Surviving Gear Ratios from Screening Test

XLEF2_1
XFLAP1_1
XFLAP2_1
XTAIL_3
XLEFA1_3
XTAIL_4
XLEFA2_4
XAILER1_4

One may notice that the gear ratio XAILER2_3 appears relatively high in the Pareto plot as a significant variable and yet is not included as a surviving variable. The reason for this is because this gear ratio corresponds to the outboard aileron for the supersonic roll. At this condition, the control surface is very ineffective, due to the flexibility of the outboard part of the wing and the high dynamic pressure at supersonic flight. The authors feel that the significance of the gear ratio of this ineffective surface may have been artificially increased during the screening test. Since each row in the DOE is an optimization, it is possible that not every case converged to a global optimum, and as a result this effect may have been inflated. Thus, it is important to scrutinize the results of the screening test and make sure that all significant effects make physical sense. In addition, this scenario highlights the need to make sure that each case has reached a global optimum. This will be particularly important in the next section as models are built of the design space.

Response Surface Equation

With the size of the problem now reduced, the next step is to build RSEs of the responses of interest (Table 5) as a function of the 8 remaining gear ratios. The methodology to create a RSE is similar to that of the screening test in that a DOE is created, responses of interest calculated for each case and inserted into the appropriate columns, and a regression analysis performed on the data. The difference, however, is the screening model is linear, whereas for the RSE it is quadratic. As a result the DOE must test the design variables not at two levels as in the screening test but at three or more levels to capture quadratic effects.

A 145 case face-centered central composite design for 8 design variables was chosen as the DOE for RSE generation. A sample of the DOE is shown in Table 8 where the -1's and +1's stand for the minimum and maximum values of the gear ratios, respectively, and 0 is the midpoint of the gear ratio within its range.

Once again, each of the rows of the DOE table refers to an ASTROS optimization with a different set of gear ratio values for every case. However, unlike the screening test, wing weight is not the only response that is extracted. In addition to weight, the other responses of interest (drag, hinge moments) are extracted and inserted into the response columns. Table 8 shows a few of the responses for which RSEs are constructed.

It must also be emphasized again that every row corresponds to a unique structural design. These unique designs are defined by the thickness of the composite plies over the wing skin. Since the next phase in the study involves evaluating the robustness of each structure, the structural designs for each case are saved in text files for future use. The *Design* column in Table 8 illustrates that for every DOE case a different structural design exists.

For each of the responses, a standard least squares regression in JMP is performed on the data and a RSE generated. A few of the more important of these RSEs are displayed in Figure 6. This plot, generated within JMP, is known as a prediction profile, and it provides the designer with a convenient means to gain visibility of the design space as modeled by the RSEs. As the designer changes the values of the gear ratios, he can immediately see the influence of the decision on the responses.

Table 8 - Sample of RSE DOE

	XLEF2_1	XFLAP1_1	XFLAP2_1	...	XLEFA2_4	XAILER1_4	Weight	Drag1	HM_AILER2_4	Design
Case 1	-1	-1	-1	...	-1	-1	359.4	20166.3	-29519.0	t1
Case 2	-1	-1	-1	...	1	1	324.0	19831.4	-12483.5	t2
Case 3	-1	-1	-1	...	-1	1	319.4	19893.0	-9904.2	t3
Case 4	-1	-1	-1	...	1	-1	320.9	19763.9	-12802.9	t4
. .	. .	. .	. .	. .	. .	. .	. .	. .	. .	. .
Case 142	0	0	0	...	1	0	295.4	20454.9	-13057.0	t142
Case 143	0	0	0	...	0	-1	310.8	20533.3	-18700.6	t143
Case 144	0	0	0	...	0	1	295.5	20479.1	-11428.1	t144
Case 145	0	0	0	...	0	0	298.2	20521.3	-13928.1	t145

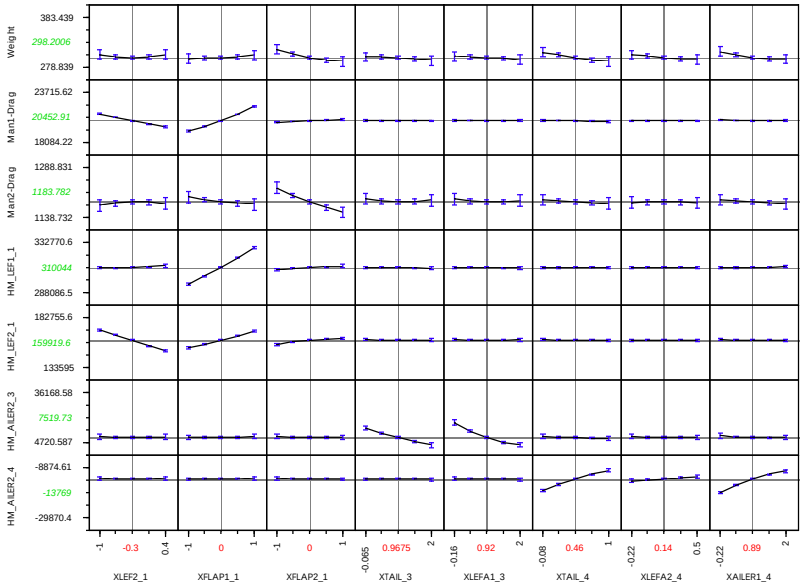

Figure 6 - Sensitivities of Responses to Gear Ratios

The prediction profile is only as good as the RSE behind it, so as a result, it is important to check the fit of the RSE to the data that was used to create it. The parameter that best quantifies the fit of the equation is the R^2 value. The R^2 measures how much of the variation in the data is being captured by the assumed model (in this case a quadratic equation). An R^2 of 1 indicates that all variation in the data is being captured by the model. Table 9 lists the R^2 values of the RSEs shown in Figure 6.

The R^2 values for the hinge moments and Drag1 are excellent, being near a perfect fit. The R^2 values for weight and Drag2 are mediocre, but not so low that the RSEs are not usable.

Table 9 - R^2 Values of Selected RSEs

Response	R^2 Value
Weight	0.9300
Drag1	0.9987
Drag2	0.9393
HM_LEF1_1	0.9983
HM_LEF2_1	0.9975
HM_AILER2_3	0.9933
HM_AILER2_4	0.9970

Another test of RSE fit is a validation test, where the response is evaluated at a number of random points throughout the design space and compared to its value as predicted by the RSE. The weight RSE is validated in Table 10 by evaluating the wing weight for 27 cases where each case corresponds to a random point in the gear ratio design space. The weight from each case is then compared to that predicted by the RSE and a percent difference calculated. Table 10 shows that the

percent difference between the actual weight and the RSE predicted weight rarely exceeds 5%. This indicates that the weight RSE is a reasonably good predictor of the exact relationship.

Table 10 - Validation Results

	Weight	Weight (RSE)	Error (Weight)
Case #1	310.27	312.18	0.61%
Case #2	302.29	294.17	-2.69%
Case #3	348.94	328.14	-5.96%
Case #4	307.03	303.29	-1.22%
Case #5	326.78	320.95	-1.79%
Case #6	301.53	306.19	1.55%
Case #7	308.91	307.45	-0.47%
Case #8	308.79	291.71	-5.53%
Case #9	303.06	309.44	2.11%
Case #10	303.98	310.91	2.28%
Case #11	342.99	342.77	-0.06%
Case #12	317.70	320.53	0.89%
Case #13	305.29	314.94	3.16%
Case #14	332.30	338.43	1.85%
Case #15	303.94	302.16	-0.59%
Case #16	320.13	329.31	2.87%
Case #17	313.48	320.49	2.24%
Case #18	302.17	297.57	-1.52%
Case #19	293.13	305.12	4.09%
Case #20	305.95	304.07	-0.62%
Case #21	321.83	312.52	-2.89%
Case #22	299.13	289.36	-3.27%
Case #23	316.41	310.27	-1.94%
Case #24	303.32	310.36	2.32%
Case #25	323.07	317.13	-1.84%
Case #26	297.79	307.62	3.30%
Case #27	313.28	315.73	0.78%

With the RSEs determined and validated, the designer, if he so chooses, could select the gear ratio values that produced the lowest weight and drag, subject to hinge moment constraints. However, this is a deterministic solution and the structural design that results from this selection in gear ratios could perform poorly if the gear ratios deviate from their chosen values. Recall, that over the course of the design process, gear ratios frequently change, so it is not unreasonable to think that deviations may occur. As a result, the next step is to evaluate each structural design resulting from each case in the DOE on its ability to meet strength requirements should the gear ratios to which it was designed be perturbed.

FPI/Robust Design

The deviations of the 8 gear ratios from their original values (values defined in each experiment of the DOE table) are modeled in FPI as probability distributions, in an attempt to anticipate the possible variation of the gear ratios over the course of the design process. With little knowledge about how the gear ratios do change over the design history, it is assumed that these probability distributions are normal with a standard deviation of 0.06. Figure 7 shows how the gear ratios for the first case of the DOE (Table 8) are modeled probabilistically. It should be noticed that the mean of each gear ratio's distribution corresponds to its value in the DOE table for that experiment.

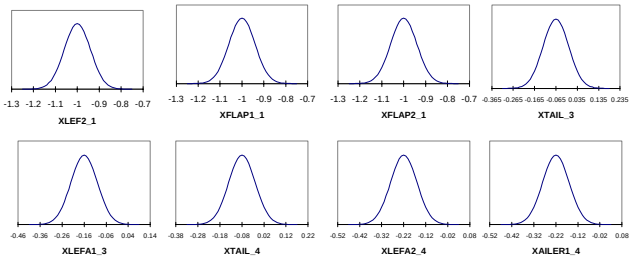

Figure 7 - Probabilistic Representation of Gear Ratios for Case #1

Since it is desired that each structural design be analyzed on its ability to be invariant to changes in the gear ratios that designed it, a function is developed that captures the magnitude of redesign should the gear ratios change. This function, which becomes the Z-function in the FPI analysis, is shown in Equation 7. The function is calculated by running an ASTROS analysis of a structural design with the gear ratios perturbed from their DOE value, and then evaluating the resulting strain constraints (allowables shown in Table 2). The strain constraints are evaluated within ASTROS by Equation 8 so that a positive constraint value means the strain allowable has been exceeded and redesign is required. In addition, the violated constraints are multiplied by a penalty function which is dependent on the number of violated constraints so that scenarios where many constraints are violated are heavily penalized.

$$F = \sum\left(\text{non} - \text{violated constraints}\right) + (\#\ \text{of violated constraints})^{0.25} \sum\left(\text{violated constraints}\right) \tag{7}$$

$$g = \frac{\varepsilon}{\varepsilon_{allowable}} - 1.0 \tag{8}$$

Using the above function and the normally distributed gear ratios as the random input variables, CDFs are generated of the function using the AMV method for each structural design of the DOE (Table 8). Figure 8 shows four arbitrarily chosen CDFs and illustrates that some of the structural designs would require less redesign than others should the gear ratios change. The invariance of a structural design is measured by looking at the function value at a probability level of 0.8 or 0.9 (F (P = 0.8 or 0.9)). The lower this function value is, the less variant the structural design.

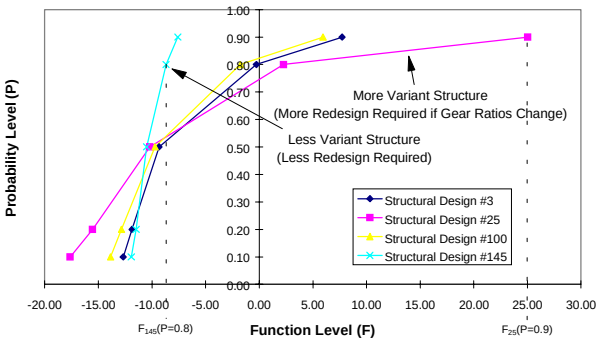

Figure 8 - Sample CDF's

response F(P=0.9) is not displayed, since its fit is not quite as good as F(P=0.8). However, it must also be acknowledged that the fit of F(P=0.8) is not particularly good, either. At an R^2 of only 0.85 the RSE cannot be used to find the one best point in the design space, but it can be used to understand trends. As a result, the designer can use these trends to find a smaller design space where both weight and variance are low and then repeat the previously described robust wing design process. With the smaller design space it is possible that a quadratic equation may prove to be a better model.

Current research is exploring ways of improving the model used for the robustness RSE. Also, ongoing work is seeking to validate the AMV method for this problem by comparing it to a Monte Carlo simulation for one case. In addition, further research into developing functions which better capture the magnitude of redesign could be of benefit.

Table 11 - DOE Table with FPI Results

	XLEF2_1	XFLAP1_1	XFLAP2_1	...	XLEFA2_4	XAILER1_4	Weight	F(P=0.8)	F(P=0.9)
Case 1	-1	-1	-1	...	-1	-1	359.4	-11.3107	-10.1091
Case 2	-1	-1	-1	...	1	1	324.0	-2.0058	5.5496
Case 3	-1	-1	-1	...	-1	1	319.4	-0.263	7.7347
Case 4	-1	-1	-1	...	1	-1	320.9	1.7651	10.4178
. .	. .	. .	. .	. .	. .	. .	. .	. .	. .
Case 142	0	0	0	...	1	0	295.4	-10.5107	-9.6926
Case 143	0	0	0	...	0	-1	310.8	-11.4272	-9.8158
Case 144	0	0	0	...	0	1	295.5	-10.3974	-9.7655
Case 145	0	0	0	...	0	0	298.2	-8.6954	-7.5848

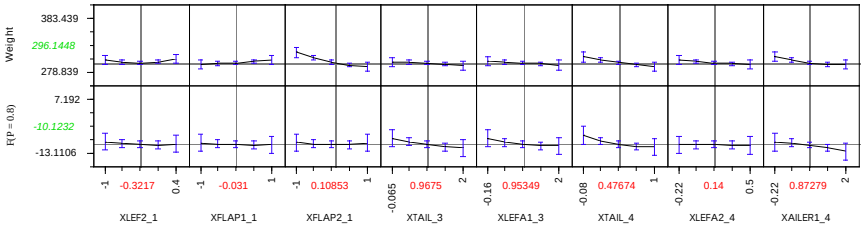

Figure 9 - Prediction Profile of FPI Results and Weight

For every CDF generated, then, the values for $F_i(P=0.8)$ and $F_i(P=0.9)$ (where i refers to the case number in the DOE table) are extracted and inserted as separate response columns into the JMP DOE table alongside weight and the other responses of interest (Table 11).

A least squares regression is then performed on the FPI responses, and a relationship generated between invariance (F(P=0.8)) and the gear ratios. It must be emphasized, however, that for the FPI responses, the designer is not controlling the actual value of the gear ratios, since as was discussed earlier there is uncertainty associated with them. Rather, the designer is controlling the *mean* of the gear ratios.

The RSEs of both weight and F(P=0.8) are displayed in Figure 9 as prediction profiles. The

Conclusions

A multidisciplinary robust wing design process applied to an aeroelastically tailored / active aeroelastic fighter configuration has been presented. The methodology incorporates the use of modal basis finite element analysis and optimization, DOE/RSM techniques, and fast probability integration in an attempt to understand the relationship between structural robustness and control surface blending. Although the assumed model of the exact relationship turned out to be poor, it did provide valuable trends which then could

be used to narrow down the design space for a second iteration.

This paper represents a first attempt at such a methodology, and ongoing work is seeking to validate both the methodology and the AMV technique, which is a key part of the methodology. In addition, it is hoped that further work will explore parametric variation of wing geometry, consider load uncertainty due to code fidelity, and consider manufacturing issues in the structural sizing process.

Acknowledgements

The authors extend thanks to: Dan Barker and Dan Egle of Lockheed Martin Tactical Aircraft Systems for their technical advice and programming assistance, Boris Moulin of Technion-Israel Institute of Technology for help in modifying ASTROS subroutines, and Daniel DeLaurentis of the Aerospace Systems Design Laboratory at Georgia Tech for help in performing the statistical analysis. Mr. Zink is supported by NASA Langley's Multidisciplinary Analysis Fellowship Program (NGT-152156). Tools are provided by Lockheed Martin Tactical Aircraft Systems under contract. Development of methodologies presented in this paper are supported by a NASA Langley Grant (NAG-1-1793).

References

1) Bohlmann, J.D, Eckstrom, C.V., and Weisshar, T.A., "Aeroelastic Tailoring for Oblique Wing Lateral Trim," Journal of Aircraft, Vol. 27, No. 6, June 1990, pp. 558-563.

2) Pendleton, E., Griffin, K., Kehoe, M., and Perry, B., "A Flight Research Program for Active Aeroelastic Wing Technology," 36th AIAA/ASME/ASCE/ AHS/ASC Structures, Structural Dynamics , and Materials Conference, April 1996.

3) DeLaurentis, D.A., Zink, P.S., Mavris, D.N., Cesnik, C.E.S., and Schrage, D.P., "New Approaches to Multidisciplinary Synthesis: An Aero-Structures-Control Application Using Statistical Techniques," 1996 World Aviation Congress, Los Angeles, CA, October 1996.

4) Mavris, D.M., and Hayden, W.T., "Probabilistic Analysis of an HSCT Modeled with an Equivalent Laminated Plate Wing," 1997 World Aviation Congress, Anaheim, CA, October 1997.

5) Neill, D.J., Johnson, E.H., and Canfield, R., "ASTROS-A Multidisciplinary Automated Design Tool," Journal of Aircraft, Vol. 27, No. 12, 1990, pp. 1021-1027.

6) Karpel, M., Moulin, B., and Love, M.H., "Modal-Based Structural Optimization with Static Aeroelastic and Stress Constraints," 36th 1995 AIAA/ASME/ASCE/AHS/ASC Structures, Structural Dynamics and Materials Conference.

7) DeLaurentis, D., Mavris, D.N., and Schrage, D.P., "System Synthesis in Preliminary Aircraft Design using Statistical Methods," 20th Congress of the International Council of the Aeronautical Sciences, Sorrento, Italy, September 1996.

8) Southwest Research Institute, FPI User's Manual and Theoretical Manual, San Antonio, TX, 1995.

9) Mavris, D.N., and Bandte, O., "Comparison of Two Probabilistic Techniques for the Assessment of Economic Uncertainty," 19th Annual Conference of the International Society of Parametric Analysts, New Orleans, LA, May 1997.

10) Mavris, D.N. and Bandte, O., "A Probabilistic Approach to Multivariate Constrained Robust Design Simulation," 1997 World Aviation Congress, Anaheim, CA, October 1997.

11) Hines, W.W., Montgomery, D.C., Probability and Statistics in Engineering and Management Science, John Wiley & Sons, Inc., New York, NY, 1990.

12) Barker, D.K. and Love, M.H., "An ASTROS Application with Path Dependent Results," AIAA/USAF/NASA/ISSMO Multidisciplinary Analysis and Optimization Conference, Bellevue, WA, September 1996.

13) Carmichael, R.L., Castellano, C.R., and Chen, C.F., The Use of Finite Element Methods for Predicting the Aerodynamics of Wing-Body Combinations, NASA SP-228, October 1969.

14) Mavris, D.N., Bandte, O., and Schrage, D.P., "Application of Probabilistic Methods for the Determination of an Economically Robust HSCT Configuration," AIAA/USAF/NASA/ISSMO Multidisciplinary Analysis and Optimization Conference, Bellevue, WA, September 1996.

15) SAS Institute Inc., JMP Computer Program and User's Manual, Cary, NC, 1994.